HHS Public Access

Author manuscript

Neurotoxicology. Author manuscript; available in PMC 2017 March 01.

Published in final edited form as:

Neurotoxicology. 2016 March ; 53: 302–313. doi:10.1016/j.neuro.2015.06.007.

Alterations in mitochondrial dynamics induced by tebufenpyrad and pyridaben in a dopaminergic neuronal cell culture model

Adhithiya Charli, **Huajun Jin**, **Vellareddy Anantharam**, **Arthi Kanthasamy**, and **Anumantha G. Kanthasamy***

Abstract

Tebufenpyrad and pyridaben are two agro-chemically important acaricides that function like the known mitochondrial toxicant rotenone. Although these two compounds have been commonly used to kill populations of mites and ticks in commercial greenhouses, their neurotoxic profiles remain largely unknown. Therefore, we investigated the effects of these two pesticides on mitochondrial structure and function in an *in vitro* cell culture model using the Seahorse bioanalyzer and confocal fluorescence imaging. The effects were compared with rotenone. Exposing rat dopaminergic neuronal cells (N27 cells) to tebufenpyrad and pyridaben for 3 h induced dose-dependent cell death with an EC_{50} of 3.98 μM and 3.77 μM, respectively. Also, tebufenpyrad and pyridaben (3 μM) exposure induced reactive oxygen species (ROS) generation and m-aconitase damage, suggesting that the pesticide toxicity is associated with oxidative damage. Morphometric image analysis with the MitoTracker red fluorescent probe indicated that tebufenpyrad and pyridaben, as well as rotenone, caused abnormalities in mitochondrial morphology, including reduced mitochondrial length and circularity. Functional bioenergetic experiments using the Seahorse XF96 analyzer revealed that tebufenpyrad and pyridaben very rapidly suppressed the basal mitochondrial oxygen consumption rate similar to that of rotenone. Further analysis of bioenergetic curves also revealed dose-dependent decreases in ATP-linked respiration and respiratory capacity. The luminescence-based ATP measurement further confirmed that pesticide-induced mitochondrial inhibition of respiration is accompanied by the loss of cellular ATP. Collectively, our results suggest that exposure to the pesticides tebufenpyrad and pyridaben induces neurotoxicity by rapidly initiating mitochondrial dysfunction and oxidative damage in dopaminergic neuronal cells. Our findings also reveal that monitoring the kinetics of mitochondrial respiration with Seahorse could be used as an early neurotoxicological high-throughput index for assessing the risk that pesticides pose to the dopaminergic neuronal system.

*To whom correspondence should be addressed: Dept. of Biomedical Sciences, Iowa State University, 2062 College of Veterinary Medicine Building, Ames, IA 50011. Tel: 515-294-2516; Fax: 515-294-2315; akanthas@iastate.edu.

Conflict of Interest

The authors have no conflicts of interest to declare.

Keywords

Tebufenpyrad; pyridaben; pesticides; neurotoxicity; mitochondrial dysfunction; oxidative stress; Seahorse

1. Introduction

A growing body of evidence suggests that exposure to neurotoxic pesticides in agricultural settings is associated with increased risk for developing Parkinson's disease (PD) (Baltazar et al., 2014, Freire and Koifman, 2012, Parron et al., 2011). Among the pesticides associated with PD, rotenone is a well-characterized inhibitor of mitochondrial complex I that occurs naturally in tropical legumes (Cabeza-Arvelaiz and Schiestl, 2012, Greenamyre et al., 2001). Experimentally, exposure to rotenone was shown to reliably produce Parkinson's-like pathology in various animal models of PD (Betarbet et al., 2000, Greenamyre et al., 2010, Johnson and Bobrovskaya, 2015, Testa et al., 2005). Furthermore, recent epidemiological evidence has linked human rotenone exposure with PD (Spivey, 2011, Tanner et al., 2011).

The pathogenic mechanisms underlying rotenone-induced Parkinsonism are not fully understood, but possibly involve inhibition of mitochondrial respiratory chains and induction of oxidative damage (Johnson and Bobrovskaya, 2015, Sherer et al., 2003). Mitochondria are pivotal to the homeostatic functioning of cells and thus the central nervous system. The primary role of mitochondria is to provide energy to cells *via* oxidative phosphorylation (Chan, 2006, Hoppins et al., 2007, Jin et al., 2014a, Zhang and Chan, 2007). Some of the critical biochemical abnormalities resulting from mitochondrial dysfunction are increased generation of reactive oxygen species (ROS), loss of ATP production during cellular respiration and impaired Ca^{2+} ion channels (Schapira, 2007, Winklhofer and Haass, 2010). Neurotoxic stress also induces structural damage to mitochondria including mitochondrial fragmentation and mitophagy (Lin et al., 2012, Lin and Beal, 2006).

Tebufenpyrad (IUPAC name: N-[(4-tert-butylphenyl)methyl]-4-chloro-5-ethyl-2-methylpyrazole-3-carboxamide) and pyridaben (IUPAC name: 2-tert-butyl-5-[(4-tert-butylphenyl)methylsulfanyl]-4-chloropyridazin-3-one) are common acaricides used to kill populations of mites and ticks in commercial greenhouses. Tebufenpyrad is chemically classified as a pyrazole carboxyamide, which is registered for use in greenhouses for the protection of ornamental plants (EPA PC Code- 090102). Pyridaben is chemically classified as a pyridazinone, whose major application is in greenhouses and vineyards (EPA PC Code-129105). Similar to rotenone, tebufenpyrad and pyridaben have been shown to function as mitochondrial complex I inhibitors (classified by the IRAC-Insecticide Resistance Action Committee - http://www.irac-online.org/modes-of-action/). Although their intended mode of action and target toxicity are similar to those of rotenone, both tebufenpyrad and pyridaben have not been studied in detail with respect to their neurotoxicity. Therefore, in this study, we evaluated the neurotoxic effects of tebufenpyrad and pyridaben in rat dopaminergic neuronal cells, with particular emphasis on their effects on mitochondrial dynamics and their roles in dopaminergic neuronal cell death.

2. Materials and Methods

2.1 Chemicals

We purchased tebufenpyrad (96% purity) from AK Scientific Inc. (Union City, CA), pyridaben (99.1% purity) from Chem Services (West Chester, PA), and rotenone (95–98% purity) and hydrogen peroxide (30 wt. % in H_2O) from Sigma (St. Louis, MO). DMSO was purchased from Fisher Scientific (Fair Law, NJ). We purchased RPMI 1640 media, fetal bovine serum (FBS), L-glutamine, penicillin, streptomycin and Sytox green nucleic acid fluorescence stain from Molecular Probes (Eugene, OR), the Muse® Count & Viability Assay Kit (Catalog # MCH100102) from EMD Millipore (Billerica, MA), and the 5-(and-6)-chloromethyl-2′,7′-dichlorodihydrofluorescein diacetate (CM-H_2DCFDA) fluorescent probe and MitoTracker red CMXROS and MitoTracker green dyes from Invitrogen (Carlsbad, CA). The Cell Titer 96® AQueous Non-Radioactive Cell Proliferation assay kit and Cell Titer Glo Luminescent Cell Viability assay kit were bought from Promega (Madison, WI). The Aconitase assay kit was purchased from Abcam (Cambridge, MA). Oligomycin, hydrogen peroxide, carbonyl cyanide 4-trifluoromethoxy-phenylhydrazone (FCCP) and antimycin A were purchased from Sigma Aldrich (St. Louis, MO), and the Seahorse FluxPak calibration solution was bought from Seahorse Biosciences (Billerica, MA).

2.2 Cell culture and treatment paradigm

The rat immortalized mesencephalic dopaminergic neuronal cell line ($1RB_3AN_{27}$, also known as N27 cells) was a kind gift from Dr. Kedar N. Prasad (University of Colorado Health Sciences Center, Denver, CO). These N27 cells have the potential to differentiate and produce dopamine in culture when exposed to a suitable cAMP triggering agent, and once the cells are differentiated they possess increased tyrosine hydroxylase (TH) expression and dopamine levels (Adams et al., 1996, Zhang et al., 2007). In this study, undifferentiated cells were grown in RPMI 1640 medium containing 10% FBS, 2 mM L-glutamine, 50 units of penicillin, and 50 μg/ml streptomycin, as described previously (Anantharam et al., 2002, Jin et al., 2011b, Prasad et al., 1998). In general, cells were plated in a tissue culture plate or flask in accordance to the experimental requirements and was cultured overnight in a humidified atmosphere of 5% CO_2 at 37°C. The cell density plated for each experiment has been provided in the methods section. The cells were treated with the specified concentrations of tebufenpyrad and pyridaben for 0–3 h in serum-free RPMI media. For all experiments with N27 cells, treatments were performed when the cells were 65–70% confluent. The pesticides tebufenpyrad and pyridaben are lipophilic in nature and are hence dissolved in DMSO. In the ROS generation and aconitase activity experiments, cells were treated with 100 μM H_2O_2 for 45 min as a positive control. Similarly, 1 μM rotenone for 3 h was used as a positive control in the SYTOX Green assay, Muse Annexin V/7-AAD assay, ATP production, and the mitochondrial dysfunction and damage studies.

2.3 MTS cell viability assays

Cell viability was measured using the Cell Titer 96® AQueous Non-Radioactive Cell Proliferation (MTS assay) kit from Promega as described previously (Jin et al., 2014b). Briefly, N27 cells were plated at 0.8×10^4 cells/well in 96-well plates one day before

treatment. The next day cells were treated in serum-free RPMI media with different concentrations of tebufenpyrad or pyridaben (0, 1, 2, 3, 5, 7, 9, 10 and 30 μM) for a time period of 3 h. Following treatment, 10 μl of MTS solution reagent mix was added to each plate well and incubated at 37°C for 45 min. At the end of incubation, the formazan crystals that formed in the live cells were dissolved by adding 25 μl of DMSO to each well. Finally, readings were taken at a wavelength of 490 nm and another reference reading for each well was taken at 670 nm to eliminate background. The data were then plotted as a dose-response curve (depicting the EC_{50}) using Prism 4.0 (GraphPad Software, San Diego, CA).

2.4 SYTOX Green cytotoxicity assays

Cell death after exposing the N27 cells to 3 μM of tebufenpyrad or pyridaben was determined using the SYTOX Green cytotoxicity, as previously described (Jin et al., 2011a, Latchoumycandane et al., 2011). The SYTOX green dye only permits dead cells to produce green fluorescence. In brief, N27 cells were grown in 24-well cell culture plates (4×10^4 cells/well) and treated with 3 μM of tebufenpyrad or pyridaben along with 1 μM SYTOX Green dye for 3 h. Fluorescent images were then taken using fluorescence microscopy (Cytation 3, Biotek, Winooski, VT) that was coupled with a 40X objective and Gen5 imaging software. For further validation, the green fluorescence was quantitatively measured at an excitation wavelength of 485 nm and an emission wavelength of 538 nm with the use of a fluorescence microplate reader (Cytation 3, Biotek).

2.5 Annexin V/7-AAD apoptosis assay

The cytotoxic effects of tebufenpyrad and pyridaben on N27 cells were also analyzed with the Annexin V/7-AAD assays using the Muse® Annexin V and Dead Cell Assay kit from Millipore (Billerica, MA). Annexin V, which is membrane permeable, labels all cells containing a nucleus. The second component of the kit is 7-AAD, which stains the membrane of the cells that have been compromised and are dying or dead. This synergistic functioning of the two components differentiates between cell populations based on their health (Khan et al., 2012, Marusiak et al., 2014). The assay was performed according to manufacturer's protocol. Briefly, N27 cells were grown in 6-well culture plates (3×10^5 cells/well) and treated with 3 μM of tebufenpyrad or pyridaben for 3 h. Following the treatment, cells were pelleted and then resuspended in 100 μl of complete growing media, followed by adding 100 μl of Muse Annexin V and Dead Cell Reagent to each tube. The tubes were mixed thoroughly and then incubated at room temperature for 20 min without light exposure. After incubation, the tubes were read individually using Muse™ Cell Analyzer (0500-3115, Millipore). Default gate settings were used to distinguish the cells in the live, early-apoptotic, late-apoptotic and dead categories.

2.6 ATP production measurement

ATP was measured using the Cell Titer Glo Luminescent Cell Viability assay kit, according to the manufacturer's instructions. N27 cells (0.8×10^4 cells/well) were seeded in a black opaque-walled 96-well cell culture plate with transparent top and bottom. Following the treatments with tebufenpyrad (3 μM) and pyridaben (3 μM) for 3 h, the plates were equilibrated for 15 min at room temperature. Once this process was completed, an equal volume of CellTiter-Glo ®Reagent was added to match the volume of media in each well.

The plates were uniformly mixed to lyse the cells and were incubated at room temperature for 30 min to stabilize the luminescence signal, which was recorded by setting the integration time to around 0.25–1 sec per well.

2.7 Measurement of ROS generation

ROS generation was measured using the CM-H_2DCFDA fluorescent probe as previously described (Ghosh et al., 2007, Gordon et al., 2010) with minor modifications. The N27 cells were grown (0.8×10^4 cells/well) in a 96-well culture plate and the treatments were carried out with tebufenpyrad (3 μM) and pyridaben (3 μM) for 3 h. Briefly, CM-H_2DCFDA was added at a final concentration of 10 μM into each treatment well to incubate with the toxicants. By following this procedure, the dye gets completely bound to the generated ROS and loaded into the cell. After the treatment, cells were washed with Hank's Buffered Salt Solution (HBSS) containing calcium and magnesium to remove the toxicants and excess dye. Fluorescence was measured using a fluorescence plate reader (excitation 488 nm and emission 515 nm).

2.8 Aconitase activity assay

An aconitase activity assay kit from Abcam was used to measure mitochondrial aconitase (m-aconitase) activity levels. N27 cells were grown (1×10^6 cells/flask) in a T25 cell culture flask and were exposed to tebufenpyrad (3 μM) and pyridaben (3 μM) for 3 h. In brief, cells were collected after treatment and resuspended in the supplied assay buffer on ice followed by centrifugation at 2000 × g for 5 min at 4°C. The resulting supernatant was collected and further centrifuged at 20,000 × g for 15 min to collect the mitochondrial fraction. The pellet was thoroughly mixed with 100 μl of ice-cold assay buffer and sonicated for 15 sec at 4°C. The lysate was then used to measure aconitase activity as per the manufacturer's protocol. Measurements were made at a wavelength of 450 nm using a microplate reader. The OD values were normalized to the protein concentration of each sample and the results were expressed as percentage control.

2.9 Mitochondrial dysfunction assay

Cells were grown (4×10^4 cells/well) in a 24-well culture plate and were treated with tebufenpyrad (3 μM) and pyridaben (3 μM) for 3 h. After treatment, the media was removed and 300 μl of 200 nM MitoTracker green dye diluted in serum-free RPMI media was added into each well and incubated at 37°C for 15 min. Following incubation, a microplate reading was taken at an excitation wavelength of 485 nm and an emission wavelength of 520 nm.

2.10 Mitochondria structural depiction assay/Imaging

N27 cells were grown (4×10^4 cells/well) in a 24-well culture plate on coverslips pre-coated with poly-D-lysine. Following treatment with tebufenpyrad (3 μM) and pyridaben (3 μM) for 3 h, cells were washed carefully once with PBS. Then 300 μl of 200 nM CMXROS MitoTracker red dye diluted in serum-free RPMI media was added and incubated at 37°C for 12 min. After incubation, wells were gently washed with PBS 3 to 5 times and then fixed in 4% paraformaldehyde (PFA) for 30 min. The wells were washed with PBS three times and the coverslips were mounted onto glass slides for microscopic imaging using a confocal

microscope (model TE2000-U, Nikon) with 60X magnification. Image analysis used in the mitochondria structural depiction assays was performed using ImageJ. Quantification of mitochondrial parameters such as mitochondrial length and degree of circularity was accomplished using a macro text file plug-in for ImageJ (Dagda et al., 2009). For analyzing the images, 6 images per group were quantified and two separate experiments were performed.

2.11 Measurement of mitochondrial oxygen consumption by Seahorse XF96 analyzer

Mitochondrial oxygen consumption was measured using a Seahorse XF96 Extracellular Flux analyzer (Seahorse Bioscience, North Billerica, MA) at the Dr. Balaraman Kalyanaraman's laboratory (Medical College of Wisconsin, Milwaukee) as described previously (Dranka et al., 2011, Dranka et al., 2012). The Seahorse XF96 Extracellular Flux analyzer is a sensitive, high-throughput instrument that makes real-time measurements of respiration rates of cells with or without oxidative stress. In our studies, we employed two different strategies to monitor the effects of tebufenpyrad and pyridaben on oxygen consumption rates (OCR) in N27 cells. One was the direct injection strategy to test the instantaneous effect on oxygen consumption rates (OCR) in N27 cells immediately after tebufenpyrad and pyridaben injections, and the other was to analyze the mitochondrial bioenergetics of N27 cells after incubation with tebufenpyrad and pyridaben by measuring the OCR at different stages. N27 cells were seeded at a density of 2×10^4 per well into a V7-PS culture plate and incubated overnight in 5% CO_2 at 37°C. For the direct injection method, the Seahorse Flux Pak cartridge was equilibrated using the equilibration buffer for one hour and then carefully loaded with different concentrations of tebufenpyrad or pyridaben (0.5, 1, 3 and 6 μM). Following this process, the V7-PS culture plate cover was replaced with the Flux Pak cartridge and the plate was loaded into the Seahorse XF96 analyzer for direct injection. For the mitochondrial bioenergetics method, cells were first treated with different concentrations of tebufenpyrad or pyridaben (0.5, 1, 3, 6 μM) for 3 h in 5% CO2 at 37°C. During this time, the Seahorse FluxPak cartridge was equilibrated and the corresponding injection ports were loaded with the mito-stressor agents oligomycin (1 μg/ml), FCCP (1 μM) and antimycin A (10 μM). Once the mito-stressors were loaded in their corresponding position in the cartridge, the treated plate was introduced into the Seahorse analyzer covered with the Flux Pak cartridge. The analyzer was then programmed to measure the basal OCR readouts in five specified time intervals before progressing to inject the mito-stressors. These stressors were injected after every three cycles of measuring OCR (Fig. 7A). Further calculations of ATP-linked respiration and respiratory capacity were performed as described (Dranka, Benavides, 2011, Dranka, Zielonka, 2012).

2.12 Statistical analysis

All statistical data analyses were performed using Prism 4.0 (GraphPad Software, San Diego, CA). The EC50 for each of the two pesticides tebufenpyrad and pyridaben was determined from the dose-response curve generated by Prism 4.0. Data were analyzed using one-way ANOVA with the Tukey-Kramer post-test for comparing all treatment groups with that of the control. Differences with $p < 0.05$ were considered significant.

3. Results

3.1 Tebufenpyrad and pyridaben treatments elicit significant neurotoxic response in the N27 dopaminergic neuronal cells

The effect of the two pesticides tebufenpyrad and pyridaben on the viability of N27 dopaminergic neuronal cells was evaluated by the MTS cell viability assay. An N27 culture comprises a homogenous population of TH-positive dopaminergic neuronal cells derived from the rat's mesencephalic region and are widely used as a versatile model of dopaminergic neurodegeneration (Anantharam, Kitazawa, 2002, Harischandra et al., 2014, Levesque et al., 2010). To generate dose-response curves, N27 cells were treated with increasing concentrations of tebufenpyrad or pyridaben (0–30 μM) for time periods of 3 h each. These 3-h treatments with tebufenpyrad or pyridaben resulted in concentration-dependent cytotoxicity in N27 cells (Figs. 1A–B). It is noteworthy that these two pesticides have similar neurotoxic effects on N27 cells with EC_{50} values of 3.98±0.21 μM (95% CI) and 3.77±0.21 μM (95% CI) for tebufenpyrad and pyridaben, respectively.

To further substantiate the cytotoxic effects of the two pesticides on N27 cells, we treated N27 cells with 3 μM of tebufenpyrad or pyridaben for 3 h and measured cell death using the SYTOX Green cytotoxicity and Muse Annexin V/7AAD assays. As a positive control, we treated N27 cells with 1 μM rotenone for 3 h. The SYTOX Green dye is a nuclear-specific probe that is excluded from cells with intact membranes, while it binds the nucleic acids of cells that have damaged membranes (Asaithambi et al., 2014, Roth et al., 1997, Sherer, Betarbet, 2003). Similar to rotenone, exposure to tebufenpyrad or pyridaben led to significantly greater toxicity in N27 cells than in control cells (Fig. 1C). Consistent with this, quantification of cell cytotoxicity using the Muse Annexin V/7AAD assay revealed significant loss of cell viability occurring in the cells treated with tebufenpyrad or pyridaben compared to the control cells (Fig. 1D). A similar toxicity was observed with the rotenone-treated positive control cells. Moreover, the Muse Annexin V/7AAD assay also showed that cells undergo apoptotic cell (Fig. 1D). Collectively, these data clearly indicate that tebufenpyrad and pyridaben induce neurotoxic effects in N27 dopaminergic neuronal cells. Based on these results, we chose a working concentration of 3 μM for both tebufenpyrad and pyridaben treatments in subsequent experiments.

3.2 Tebufenpyrad and pyridaben induce oxidative damage

To explore the role of oxidative stress in tebufenpyrad- and pyridaben-induced neurotoxicity, we first examined the effect of tebufenpyrad and pyridaben on intracellular ROS generation. N27 cells were treated with vehicle, tebufenpyrad or pyridaben for 30, 60, and 180 min and the rate of ROS generation was quantified using the CM-H2DCFDA fluorescent probe. Hydrogen peroxide was used as a positive control in the experiment. Both tebufenpyrad and pyridaben, at a concentration of 3 μM, induced a time-dependent increase in ROS production, starting as early as 30 min (Figs. 2A–B). At 180 min, both pesticides induced approximately a 3-fold increase of ROS levels. These results suggest that ROS generation might be an early biochemical change that precedes cell death following tebufenpyrad and pyridaben exposure in dopaminergic neuronal cells. To further characterize the involvement of oxidative stress in tebufenpyrad and pyridaben

neurotoxicity, we performed m-aconitase activity assays. Aconitase is a mitochondrial protein that catalyzes the conversion of citrate to isocitrate in the TCA cycle. This enzyme complex has an iron sulfur cluster that is very sensitive to oxidative damage (Ghosh et al., 2010, Kalyanaraman, 2013). The loss of aconitase enzyme activity is commonly used as a measure of mitochondrial oxidative damage (Cantu et al., 2009). We observed significant reductions of m-aconitase activity in cells treated with tebufenpyrad and pyridaben (Fig. 3). Hydrogen peroxide, as a positive control, produced similar results. Together, these data indicate that tebufenpyrad and pyridaben induce oxidative damage to mitochondria in dopaminergic cells.

3.3 Tebufenpyrad and pyridaben significantly induce mitochondrial structural damage and dysfunction in dopaminergic neuronal cells

To gain further insight into the mechanisms underlying tebufenpyrad- and pyridaben-induced dopaminergic cell death, we studied their effects on mitochondrial function. We first monitored mitochondrial function by using the cell-permeable mitochondria-selective dye MitoTracker green, which passively diffuses across the plasma cell membrane and accumulates in active mitochondria. Treatments with tebufenpyrad and pyridaben led to about a 40% loss of MitoTracker green fluorescence when compared to control cells (Fig. 4), strongly suggesting the loss of mitochondrial function.

To visualize the structural abnormalities of mitochondria following tebufenpyrad and pyridaben exposure, we performed a detailed confocal microscopic analysis using MitoTracker red dye in N27 dopaminergic cells. Mitochondria from control cells appeared as long, thread-like structures that were well-linked and randomly distributed throughout the cells. However, in the tebufenpyrad- and pyridaben-treated groups, they appeared as disintegrated circular structures that were not connected or linked to one another (Fig. 5A), indicative of mitochondrial fission. Using ImageJ analysis, we quantified structural features including mitochondrial length (Fig. 5B) and mitochondrial circularity (Fig. 5C). In contrast to the control group, the mitochondria in tebufenpyrad- and pyridaben-treated cells were significantly shorter and more circular, further indicating a striking loss of mitochondrial structural integrity post-exposure. Collectively, our data suggest that tebufenpyrad and pyridaben exposure induces a profound structural impairment to mitochondria in dopaminergic neuronal cells.

3.4 Tebufenpyrad and pyridaben reduce oxygen consumption rates and increase mitochondrial stress levels

After demonstrating that tebufenpyrad and pyridaben induce mitochondrial impairment, we directly measured mitochondrial oxygen consumption rates and stress levels over time following pesticide exposure. We employed the Seahorse mitochondrial analyzer to perform two different sets of experiments. One set involved the direct injection method (Figs. 6A) after the measurement of basal respiration, which helped us to assess the effects of tebufenpyrad and pyridaben on the instantaneous respiration rate of dopaminergic neuronal cells. The second set of experiments, using the Seahorse analyzer post-pesticide treatment, involved measuring key parameters of mitochondrial bioenergetics (Fig. 7A) including basal respiration, ATP-linked respiration and respiration capacity.

To study the dose-response effect on respiration rates immediately after the direct injection process, we injected N27 dopaminergic cells with 0.5, 1, 3 and 6 μM of tebufenpyrad and pyridaben, both of which dose-dependently affected respiration rates (Figs. 6B and C). The lowest concentration of 0.5 μM tebufenpyrad did not affect baseline respiration rates significantly. However, the 1, 3 and 5 μM doses of tebufenpyrad significantly decreased the respiration rate immediately following exposure to the pesticide. The pyridaben treatment produced a much more detrimental effect on mitochondrial respiration. Even its lowest dose of 0.5 μM induced a steep decrease in baseline respiration, and this effect continued to worsen at higher exposure concentrations (Fig. 6C). Thus, pyridaben has a more potent effect than tebufenpyrad on mitochondrial respiration rate in dopaminergic neuronal cells.

Measuring mitochondrial respiration kinetics with the Seahorse analyzer allowed us to determine the effect of toxic agents on the three critical stages of respiration. The first stage involves the addition of an ATP synthase inhibitor, oligomycin, which suddenly decreases the oxygen consumption rate (OCR). The next stage is the addition of FCCP, which acts as an uncoupler that increases mitochondrial oxygen consumption by disinhibiting the flow of protons across the mitochondrial inner membrane due to uncoupling of the electron transport chain. The final stage is the addition of antimycin A, which is a respiratory chain inhibitor that shuts down mitochondrial activity completely. After exposing N27 cells to different concentrations of tebufenpyrad (0.5, 1, 3 and 6 μM) and running the bioenergetics stages, we calculated ATP-linked respiration and respiratory capacity (Dranka et al., 2010, Jekabsons and Nicholls, 2004). As depicted in the Seahorse bioenergetics map (Fig. 7A), tebufenpyrad-treated cells revealed dramatic changes in all three stages of mitochondrial respiration in contrast to control cells. Quantitative analysis showed a dose-dependent decrease in basal respiration, ATP-linked respiration and respiratory capacity produced by tebufenpyrad. At the higher doses of 3 and 6 μM tebufenpyrad, mitochondrial oxygen consumption did not recover following FCCP treatment, indicating that these dose ranges produce irreversible damage to mitochondrial function (Figs. 7B–E). Similarly, pyridaben exposure (0.5, 1, 3 and 6 μM for 3 h) also produced a dose-dependent decrease in basal respiration, ATP-linked respiration and respiratory capacity, which were all exceedingly low for all doses of pyridaben (Figs. 7F–I). Comparing the bioenergetics data of tebufenpyrad and pyridaben showed that pyridaben was more potent than tebufenpyrad. Collectively, these results show that both tebufenpyrad and pyridaben profoundly impair mitochondrial respiration in dopaminergic neuronal cells.

3.5 Tebufenpyrad and pyridaben deplete intracellular bioenergy levels in dopaminergic neuronal cells

To further confirm that tebufenpyrad- and pyridaben-induced mitochondrial inhibition reduces cellular biogenetics, we employed a highly sensitive luminescence-based assay to assess the cellular ATP content in N27 neuronal cells. The cells were treated with 3 μM tebufenpyrad or pyridaben for 3 h. We used 1 μM rotenone as a positive control under the same experimental conditions, since it is a potent agent for shutting down mitochondria and disrupting the electron transport chain (ETC) (Sherer et al., 2007). Both tebufenpyrad and pyridaben dramatically depleted intracellular ATP in dopaminergic neuronal cells (Fig. 8). The positive control rotenone also reduced cellular ATP content. These results suggest that

tebufenpyrad and pyridaben exposure induces severe energy deficits resulting from mitochondrial impairment in dopaminergic neuronal cells.

4. Discussion

Our study clearly demonstrates that the two greenhouse pesticides tebufenpyrad and pyridaben exert noteworthy neurotoxic effects on dopaminergic neuronal cells. Systematic characterization of the toxicological mechanisms underlying tebufenpyrad and pyridaben neurotoxicity reveals that these pesticides disrupted mitochondrial dynamics by inducing severe structural, functional, and oxidative damage. Our present study provides strong evidence that tebufenpyrad and pyridaben induce neurotoxicity by targeting mitochondrial structure and function in dopaminergic neuronal cells.

Tebufenpyrad and pyridaben are widely used pesticides in greenhouses and vineyards. Despite their widespread use, the potential neurotoxic effects of these compounds on the dopaminergic neuronal system are not well studied. But a recent study has reported that pyridaben exposure induced a 24% TH neuronal loss in the substantia nigra (SN) of mice. The authors also performed an RNAseq analysis and reported that mice exposed to certain pesticides exhibited gene expression patterns bearing significant correspondence to pathways that were well-known in human PD cases (Gollamudi et al., 2012). The results reported above have important implications about the neurotoxicological effects that tebufenpyrad and pyridaben might have on animal and human dopaminergic neuronal systems. In the present study, we used the MTS viability assay to calculate EC_{50} values of 3.98 and 3.77 μM for tebufenpyrad and pyridaben, respectively (Figs. 1A–B). Further cytotoxicity studies using the SYTOX Green and Muse Annexin V/7-AAD assays revealed that tebufenpyrad and pyridaben at a concentration of 3 μM elicit a similar toxicity to that of rotenone (1 μM) in N27 cells (Figs. 1C–D). An overview study using bovine and rat mitochondria demonstrated the mitochondrial complex I-specific inhibitory actions of tebufenpyrad and pyridaben with respect to their potency as it related to rotenone (Degli Esposti, 1998). Adding on, the cytotoxicity trend in SK-N-MC human neuroblastoma cells has previously been shown to be: pyridaben > rotenone > tebufenpyrad (Sherer, Richardson, 2007). In our study, exposing N27 dopaminergic neuronal cells to tebufenpyrad or pyridaben showed similar inhibitory effects on mitochondrial respiration, ATP production and oxidative damage. Variation in the toxicity and the effects of mitochondrial dysfunction induced by tebufenpyrad and pyridaben in different studies might be based on cell type, their species of origin, the organ of localization of the cells to which the pesticides are targeted and other factors such as concentrations and duration of treatment. The results from MTS and ATP production assays also showed that these environmental toxicants cause significant dopaminergic neuronal cell death at certain doses and durations of exposure. Clearly, further investigations examining exposure routes and risk levels *in vivo* are needed to better understand the environmental risk posed by these two compounds. Another noteworthy result contributing to the significant dopaminergic toxicity of tebufenpyrad and pyridaben was the rapid, time-dependent generation of reactive oxygen species (Fig. 2). Additionally, tebufenpyrad and pyridaben treatments reduced m-aconitase activity (Fig. 3), which is a clear sign of oxidative damage instigated by the production of superoxides (Gardner, 2002). M-aconitase is a major iron-sulfur enzyme that has been used as a marker of oxidative

damage following various neurotoxic chemical exposures including pesticides (Cantu, Schaack, 2009, Drechsel and Patel, 2008). To our knowledge, this is the first report demonstrating the sensitivity of mitochondrial aconitase to the greenhouse pesticides tebufenpyrad and pyridaben.

Both tebufenpyrad and pyridaben are considered to be mitochondrial inhibitors (by IRAC). Our experimental evidence supports this classification by demonstrating the potent effects of the pesticides on mitochondria in dopaminergic neuronal cells. Exposure of N27 cells to tebufenpyrad and pyridaben for 3 h induced a remarkable loss of mitochondrial function and ATP production (Figs. 4 and 8). Similar studies with other complex-1 inhibitors such as rotenone have been shown to cause PD-like symptoms through neuronal loss and apoptosis (Greenamyre, Sherer, 2001). We microscopically observed a clear structural morphological change in the mitochondria after exposure to tebufenpyrad and pyridaben when compared to the healthy control group (Fig. 5). This provided clear evidence of structural damage occurring apart from the mitochondrial dysfunction induced by the greenhouse toxicants. Thus, tebufenpyrad and pyridaben are both potently able to cause extensive mitochondrial damage leading to dopaminergic neuronal cell death. These results advance our understanding of the detrimental effects of tebufenpyrad and pyridaben as mitochondrial complex-1 inhibitors in inducing selective neuronal damage to the nigrostriatal dopaminergic system similar to rotenone exposure in animal models. Our analysis of mitochondrial respiration kinetics using the high-throughput Seahorse XF96 analyzer provided valuable information regarding the extent of the mitochondrial dysfunctional response to these pesticides. The Seahorse Bioanalyzer facilitates the precise measurement of oxygen consumption rates of intact live cells using a set of highly sensitive and specialized electrodes. This makes it a high-throughput system requiring a minimal number of cells and is also more efficient when compared to the traditional polarographic methods (Dranka, Benavides, 2011, Rogers et al., 2011, Sauerbeck et al., 2011). Direct injection of the pesticides using the Seahorse XF96 analyzer clearly showed an instantaneous reduction in respiration rates after exposing N27 dopaminergic cells to different concentrations of tebufenpyrad and pyridaben (Figs. 6A–C). Further analysis of Seahorse respiration curves revealed that the pesticides induced severe mitochondrial stress characterized by impaired basal respiration, ATP-linked respiration and respiratory capacity (Fig. 7). Notably, the Seahorse analyzer findings revealed pyridaben to be more potent than tebufenpyrad even at lower doses, suggesting that analysis of mitochondrial function by the high-throughput Seahorse system will be an invaluable tool to determine rank-order potency of pesticides having potential mitochondrial toxicity. Incorporating such analyses in pesticide development will minimize the off-target toxicity to the human nervous system. Overall, our study provides pivotal neurotoxicological data demonstrating that these two neurotoxicants cause significant damage to the dopaminergic neuronal oxygen consumption system, thereby leading to significant mitochondrial dysfunction and oxidative damage.

A very recent report by the Washington State Department of Agriculture (WSDA) stated that there were 20 farm workers working in a cherry orchard who had been poisoned by an off-target exposure to a mixture of pesticides that were being applied in a neighboring pear orchid. Interestingly, one of the components of the pesticide mixture was revealed to be pyridaben. The affected farmers were medically treated for neurological, respiratory, ocular

and gastrointestinal symptoms (Calvert et al., 2015). In terms of human exposure studies in greenhouse settings, female workers exposed to an organophosphate exhibited longer reaction times and reduced motor stability when compared to an unexposed group of women. Adding to these symptoms, the affected group also suffered from depression, hypertension and fatigue (Bazylewicz-Walczak et al., 1999). A 2006 study of the school children of greenhouse workers in Ecuador demonstrated a long-term maternal effect from prenatal exposure to greenhouse pesticides causing deficits in their motor coordination and visual memory (Grandjean et al., 2006). The evidence from these greenhouse epidemiological studies suggests that pesticide exposure in greenhouses might have a significant effect on the human nervous system, thereby instigating a number of neurodegenerative symptoms. Keeping in mind the neurotoxic effects of exposure to pesticides in greenhouses, the results from our experimental studies suggest that persistent exposure to complex 1 inhibitors, such as tebufenpyrad and pyridaben, represents a neurological occupational hazard that could adversely affect greenhouse workers. Since tebufenpyrad and pyridaben have a terrestrial field dissipation half-life of about 50 and 11 days, respectively (TOXNET and NLM - CASRN: 119168-77-3 and CASRN: 96489-71-3), persistent exposure in closed environments such as a greenhouse setting likely poses a risk to humans. Several screening methodologies using cell model systems have been explored recently for rapid identification of adverse effects of environmental pesticide contaminations (Heusinkveld et al., 2014, Meijer et al., 2014).

In summary, we report here an interesting finding that the neurotoxic effects of tebufenpyrad and pyridaben are mainly manifested as damage to both structural and functional aspects of mitochondria in dopaminergic neuronal cells. The extent to which these greenhouse pesticides alter the mitochondrial dynamics could be used as a marker of *in vitro* pesticide neurotoxicity. Considering the enhanced vulnerability of dopaminergic neuronal cells to mitochondrial impairment produced by tebufenpyrad and pyridaben in our study, chronic exposure to these greenhouse pesticides may have implications in environmentally-linked PD. Further studies in animal models and epidemiological studies in greenhouse workers will clarify the potential risk of greenhouse pesticides in the etiology of PD.

Acknowledgments

This work was supported by National Institutes of Health (NIH) Grants: ES10586, NS 039958 and NS074443. The W. Eugene and Linda Lloyd Endowed Chair to AGK and Deans Professorship to AK are also acknowledged. The authors would like to thank Dr. Balaraman Kalyanaraman for providing access to the Seahorse XF96 analyzer used in this study. The authors also acknowledge Mr. Gary Zenitsky for his assistance in editing this manuscript.

References

Adams FS, La Rosa FG, Kumar S, Edwards-Prasad J, Kentroti S, Vernadakis A, et al. Characterization and transplantation of two neuronal cell lines with dopaminergic properties. Neurochem Res. 1996; 21:619–27. [PubMed: 8726972]

Anantharam V, Kitazawa M, Wagner J, Kaul S, Kanthasamy AG. Caspase-3-dependent proteolytic cleavage of protein kinase Cdelta is essential for oxidative stress-mediated dopaminergic cell death after exposure to methylcyclopentadienyl manganese tricarbonyl. J Neurosci. 2002; 22:1738–51. [PubMed: 11880503]

Asaithambi A, Ay M, Jin H, Gosh A, Anantharam V, Kanthasamy A, et al. Protein kinase D1 (PKD1) phosphorylation promotes dopaminergic neuronal survival during 6-OHDA-induced oxidative stress. PLoS One. 2014; 9:e96947. [PubMed: 24806360]

Baltazar MT, Dinis-Oliveira RJ, de Lourdes Bastos M, Tsatsakis AM, Duarte JA, Carvalho F. Pesticides exposure as etiological factors of Parkinson's disease and other neurodegenerative diseases--a mechanistic approach. Toxicol Lett. 2014; 230:85–103. [PubMed: 24503016]

Bazylewicz-Walczak B, Majczakowa W, Szymczak M. Behavioral effects of occupational exposure to organophosphorous pesticides in female greenhouse planting workers. Neurotoxicology. 1999; 20:819–26. [PubMed: 10591517]

Betarbet R, Sherer TB, MacKenzie G, Garcia-Osuna M, Panov AV, Greenamyre JT. Chronic systemic pesticide exposure reproduces features of Parkinson's disease. Nat Neurosci. 2000; 3:1301–6. [PubMed: 11100151]

Cabeza-Arvelaiz Y, Schiestl RH. Transcriptome analysis of a rotenone model of parkinsonism reveals complex I-tied and -untied toxicity mechanisms common to neurodegenerative diseases. PLoS One. 2012; 7:e44700. [PubMed: 22970289]

Calvert GM, Rodriguez L, Prado JB. (CDC) CfDCaP. Worker illness related to newly marketed pesticides--Douglas County, Washington, 2014. MMWR Morb Mortal Wkly Rep. 2015; 64:42–4. [PubMed: 25611169]

Cantu D, Schaack J, Patel M. Oxidative inactivation of mitochondrial aconitase results in iron and H2O2-mediated neurotoxicity in rat primary mesencephalic cultures. PLoS One. 2009; 4:e7095. [PubMed: 19763183]

Chan DC. Mitochondria: dynamic organelles in disease, aging, and development. Cell. 2006; 125:1241–52. [PubMed: 16814712]

Dagda RK, Cherra SJ, Kulich SM, Tandon A, Park D, Chu CT. Loss of PINK1 function promotes mitophagy through effects on oxidative stress and mitochondrial fission. J Biol Chem. 2009; 284:13843–55. [PubMed: 19279012]

Degli Esposti M. Inhibitors of NADH-ubiquinone reductase: an overview. Biochim Biophys Acta. 1998; 1364:222–35. [PubMed: 9593904]

Dranka BP, Benavides GA, Diers AR, Giordano S, Zelickson BR, Reily C, et al. Assessing bioenergetic function in response to oxidative stress by metabolic profiling. Free Radic Biol Med. 2011; 51:1621–35. [PubMed: 21872656]

Dranka BP, Hill BG, Darley-Usmar VM. Mitochondrial reserve capacity in endothelial cells: The impact of nitric oxide and reactive oxygen species. Free Radic Biol Med. 2010; 48:905–14. [PubMed: 20093177]

Dranka BP, Zielonka J, Kanthasamy AG, Kalyanaraman B. Alterations in bioenergetic function induced by Parkinson's disease mimetic compounds: lack of correlation with superoxide generation. J Neurochem. 2012; 122:941–51. [PubMed: 22708893]

Drechsel DA, Patel M. Role of reactive oxygen species in the neurotoxicity of environmental agents implicated in Parkinson's disease. Free Radic Biol Med. 2008; 44:1873–86. [PubMed: 18342017]

Freire C, Koifman S. Pesticide exposure and Parkinson's disease: epidemiological evidence of association. Neurotoxicology. 2012; 33:947–71. [PubMed: 22627180]

Gardner PR. Aconitase: sensitive target and measure of superoxide. Methods Enzymol. 2002; 349:9–23. [PubMed: 11912933]

Ghosh A, Chandran K, Kalivendi SV, Joseph J, Antholine WE, Hillard CJ, et al. Neuroprotection by a mitochondria-targeted drug in a Parkinson's disease model. Free Radic Biol Med. 2010; 49:1674–84. [PubMed: 20828611]

Ghosh S, Patel N, Rahn D, McAllister J, Sadeghi S, Horwitz G, et al. The thiazolidinedione pioglitazone alters mitochondrial function in human neuron-like cells. Mol Pharmacol. 2007; 71:1695–702. [PubMed: 17387142]

Gollamudi S, Johri A, Calingasan NY, Yang L, Elemento O, Beal MF. Concordant signaling pathways produced by pesticide exposure in mice correspond to pathways identified in human Parkinson's disease. PLoS One. 2012; 7:e36191. [PubMed: 22563483]

Gordon R, Hogan CE, Neal ML, Anantharam V, Kanthasamy AG, Kanthasamy A. A simple magnetic separation method for high-yield isolation of pure primary microglia. J Neurosci Methods. 2010; 194:287–96. [PubMed: 21074565]

Grandjean P, Harari R, Barr DB, Debes F. Pesticide exposure and stunting as independent predictors of neurobehavioral deficits in Ecuadorian school children. Pediatrics. 2006; 117:e546–56. [PubMed: 16510633]

Greenamyre JT, Cannon JR, Drolet R, Mastroberardino PG. Lessons from the rotenone model of Parkinson's disease. Trends Pharmacol Sci. 2010; 31:141–2. author reply 2–3. [PubMed: 20096940]

Greenamyre JT, Sherer TB, Betarbet R, Panov AV. Complex I and Parkinson's disease. IUBMB Life. 2001; 52:135–41. [PubMed: 11798025]

Harischandra DS, Jin H, Anantharam V, Kanthasamy A, Kanthasamy AG. α-Synuclein Protects against Manganese Neurotoxic Insult during the Early Stages of Exposure in a Dopaminergic Cell Model of Parkinson's Disease. Toxicol Sci. 2014

Heusinkveld HJ, van den Berg M, Westerink RH. In vitro dopaminergic neurotoxicity of pesticides: a link with neurodegeneration? Vet Q. 2014; 34:120–31. [PubMed: 25506807]

Hoppins S, Lackner L, Nunnari J. The machines that divide and fuse mitochondria. Annu Rev Biochem. 2007; 76:751–80. [PubMed: 17362197]

Jekabsons MB, Nicholls DG. In situ respiration and bioenergetic status of mitochondria in primary cerebellar granule neuronal cultures exposed continuously to glutamate. J Biol Chem. 2004; 279:32989–3000. [PubMed: 15166243]

Jin H, Kanthasamy A, Anantharam V, Rana A, Kanthasamy AG. Transcriptional regulation of pro-apoptotic protein kinase Cdelta: implications for oxidative stress-induced neuronal cell death. J Biol Chem. 2011a; 286:19840–59. [PubMed: 21467032]

Jin H, Kanthasamy A, Ghosh A, Anantharam V, Kalyanaraman B, Kanthasamy AG. Mitochondria-targeted antioxidants for treatment of Parkinson's disease: preclinical and clinical outcomes. Biochim Biophys Acta. 2014a; 1842:1282–94. [PubMed: 24060637]

Jin H, Kanthasamy A, Ghosh A, Yang Y, Anantharam V, Kanthasamy AG. α-Synuclein negatively regulates protein kinase Cδ expression to suppress apoptosis in dopaminergic neurons by reducing p300 histone acetyltransferase activity. J Neurosci. 2011b; 31:2035–51. [PubMed: 21307242]

Jin H, Kanthasamy A, Harischandra DS, Kondru N, Ghosh A, Panicker N, et al. Histone Hyperacetylation Upregulates PKCdelta in Dopaminergic Neurons to Induce Cell Death: Relevance to Epigenetic Mechanisms of Neurodegeneration in Parkinson's Disease. J Biol Chem. 2014b

Johnson ME, Bobrovskaya L. An update on the rotenone models of Parkinson's disease: their ability to reproduce the features of clinical disease and model gene-environment interactions. Neurotoxicology. 2015; 46:101–16. [PubMed: 25514659]

Kalyanaraman B. Teaching the basics of redox biology to medical and graduate students: Oxidants, antioxidants and disease mechanisms. Redox Biol. 2013; 1:244–57. [PubMed: 24024158]

Khan A, Gillis K, Clor J, Tyagarajan K. Simplified evaluation of apoptosis using the Muse cell analyzer. Postepy Biochem. 2012; 58:492–6. [PubMed: 23662443]

Latchoumycandane C, Anantharam V, Jin H, Kanthasamy A. Dopaminergic neurotoxicant 6-OHDA induces oxidative damage through proteolytic activation of PKCδ in cell culture and animal models of Parkinson's disease. Toxicol Appl Pharmacol. 2011; 256:314–23. [PubMed: 21846476]

Levesque S, Wilson B, Gregoria V, Thorpe LB, Dallas S, Polikov VS, et al. Reactive microgliosis: extracellular micro-calpain and microglia-mediated dopaminergic neurotoxicity. Brain. 2010; 133:808–21. [PubMed: 20123724]

Lin M, Chandramani-Shivalingappa P, Jin H, Ghosh A, Anantharam V, Ali S, et al. Methamphetamine-induced neurotoxicity linked to ubiquitin-proteasome system dysfunction and autophagy-related changes that can be modulated by protein kinase C delta in dopaminergic neuronal cells. Neuroscience. 2012; 210:308–32. [PubMed: 22445524]

Lin MT, Beal MF. Mitochondrial dysfunction and oxidative stress in neurodegenerative diseases. Nature. 2006; 443:787–95. [PubMed: 17051205]

Marusiak AA, Edwards ZC, Hugo W, Trotter EW, Girotti MR, Stephenson NL, et al. Mixed lineage kinases activate MEK independently of RAF to mediate resistance to RAF inhibitors. Nat Commun. 2014; 5:3901. [PubMed: 24849047]

Meijer M, Hendriks HS, Heusinkveld HJ, Langeveld WT, Westerink RH. Comparison of plate reader-based methods with fluorescence microscopy for measurements of intracellular calcium levels for the assessment of in vitro neurotoxicity. Neurotoxicology. 2014; 45:31–7. [PubMed: 25224521]

Parron T, Requena M, Hernandez AF, Alarcon R. Association between environmental exposure to pesticides and neurodegenerative diseases. Toxicol Appl Pharmacol. 2011; 256:379–85. [PubMed: 21601587]

Prasad KN, Clarkson ED, La Rosa FG, Edwards-Prasad J, Freed CR. Efficacy of grafted immortalized dopamine neurons in an animal model of parkinsonism: a review. Mol Genet Metab. 1998; 65:1–9. [PubMed: 9787089]

Rogers GW, Brand MD, Petrosyan S, Ashok D, Elorza AA, Ferrick DA, et al. High throughput microplate respiratory measurements using minimal quantities of isolated mitochondria. PLoS One. 2011; 6:e21746. [PubMed: 21799747]

Roth BL, Poot M, Yue ST, Millard PJ. Bacterial viability and antibiotic susceptibility testing with SYTOX green nucleic acid stain. Appl Environ Microbiol. 1997; 63:2421–31. [PubMed: 9172364]

Sauerbeck A, Pandya J, Singh I, Bittman K, Readnower R, Bing G, et al. Analysis of regional brain mitochondrial bioenergetics and susceptibility to mitochondrial inhibition utilizing a microplate based system. J Neurosci Methods. 2011; 198:36–43. [PubMed: 21402103]

Schapira AH. Mitochondrial dysfunction in Parkinson's disease. Cell Death Differ. 2007; 14:1261–6. [PubMed: 17464321]

Sherer TB, Betarbet R, Testa CM, Seo BB, Richardson JR, Kim JH, et al. Mechanism of toxicity in rotenone models of Parkinson's disease. J Neurosci. 2003; 23:10756–64. [PubMed: 14645467]

Sherer TB, Richardson JR, Testa CM, Seo BB, Panov AV, Yagi T, et al. Mechanism of toxicity of pesticides acting at complex I: relevance to environmental etiologies of Parkinson's disease. J Neurochem. 2007; 100:1469–79. [PubMed: 17241123]

Spivey A. Rotenone and paraquat linked to Parkinson's disease: human exposure study supports years of animal studies. Environ Health Perspect. 2011; 119:A259. [PubMed: 21628118]

Tanner CM, Kamel F, Ross GW, Hoppin JA, Goldman SM, Korell M, et al. Rotenone, paraquat, and Parkinson's disease. Environ Health Perspect. 2011; 119:866–72. [PubMed: 21269927]

Testa CM, Sherer TB, Greenamyre JT. Rotenone induces oxidative stress and dopaminergic neuron damage in organotypic substantia nigra cultures. Brain Res Mol Brain Res. 2005; 134:109–18. [PubMed: 15790535]

Winklhofer KF, Haass C. Mitochondrial dysfunction in Parkinson's disease. Biochim Biophys Acta. 2010; 1802:29–44. [PubMed: 19733240]

Zhang D, Kanthasamy A, Yang Y, Anantharam V, Kanthasamy A. Protein kinase C delta negatively regulates tyrosine hydroxylase activity and dopamine synthesis by enhancing protein phosphatase-2A activity in dopaminergic neurons. J Neurosci. 2007; 27:5349–62. [PubMed: 17507557]

Zhang Y, Chan DC. New insights into mitochondrial fusion. FEBS Lett. 2007; 581:2168–73. [PubMed: 17331506]

Highlights

- Tebufenpyrad (TF) and pyridaben (PY) are dose-dependently toxic in dopaminergic neuronal cells.
- TF and PY impair mitochondrial respiration, O_2 consumption and ATP production.
- TF and PY induce severe mitochondrial structural abnormalities.
- Oxidative damage underlies TF and PY induced dopaminergic neurotoxicity.

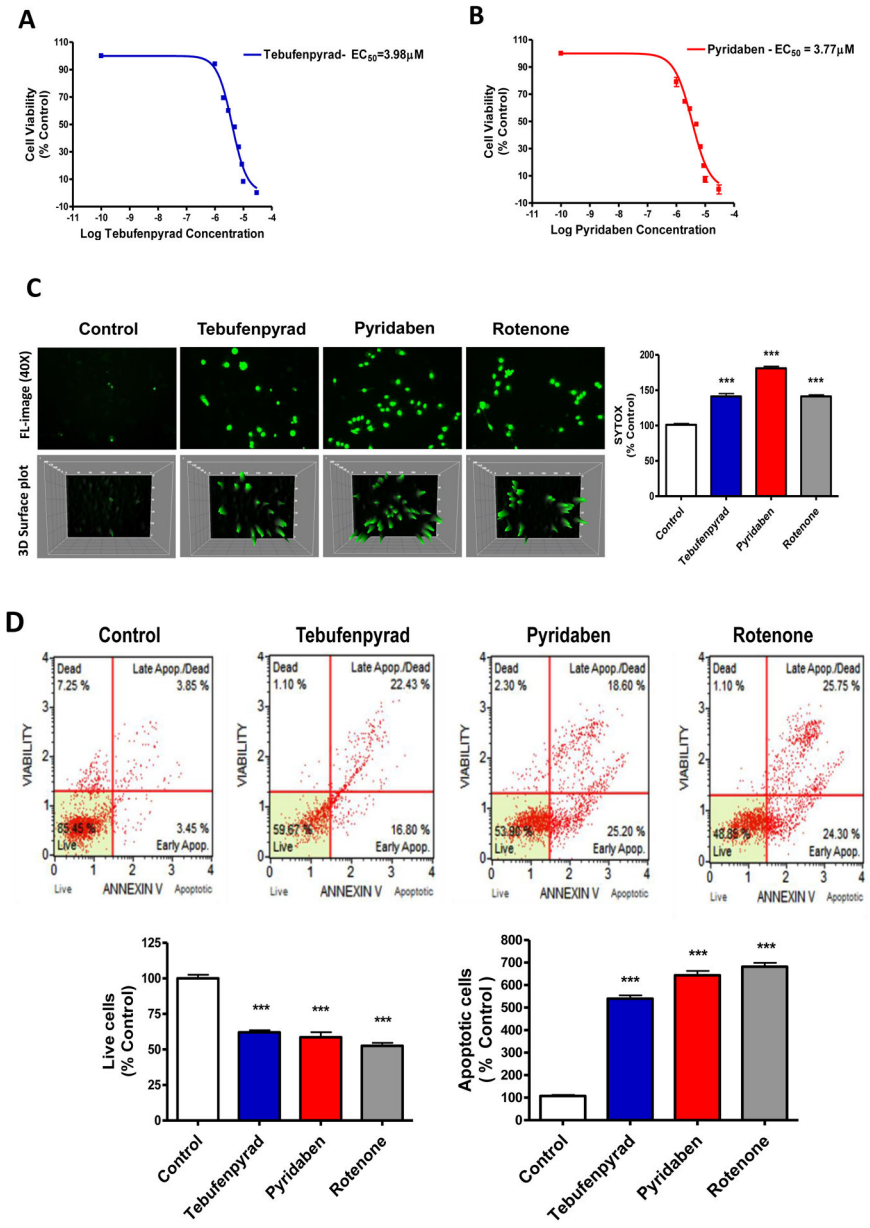

Figure 1. Dose-dependent cytotoxic effect on N27 dopaminergic neuronal cells post-exposure to tebufenpyrad and pyridaben

N27 cells were treated with varying concentrations (0, 1, 2, 3, 5, 7, 9, 10 and 30 μM) of tebufenpyrad (A) and pyridaben (B) for 3 h and then assayed for MTS cell viability, expressed as a percentage of controls. The results represent two individual experiments performed in octuplicate. (C) The N27 cells were treated with tebufenpyrad (3 μM) and pyridaben (3 μM) for 3 h, and the cytotoxic effect was measured using SYTOX Green assays. Representative SYTOX Green staining images are shown. The top view of the SYTOX Green images is also shown as a 3D surface plot in the left bottom panel. Asterisks ***$p < 0.001$ for control versus pesticide-treated groups. The results represent the mean ± S.E. of two individual experiments performed in quadruplicate. (D) Muse Annexin V/7-AAD assays were additionally performed to measure the cytotoxicity of tebufenpyrad (3

μM) and pyridaben (3 μM) for 3 h on N27 cells. Asterisks ***$p < 0.001$ for control versus pesticide-treated groups. The results represent the mean ± S.E. of two separate experiments performed in quadruplicate.

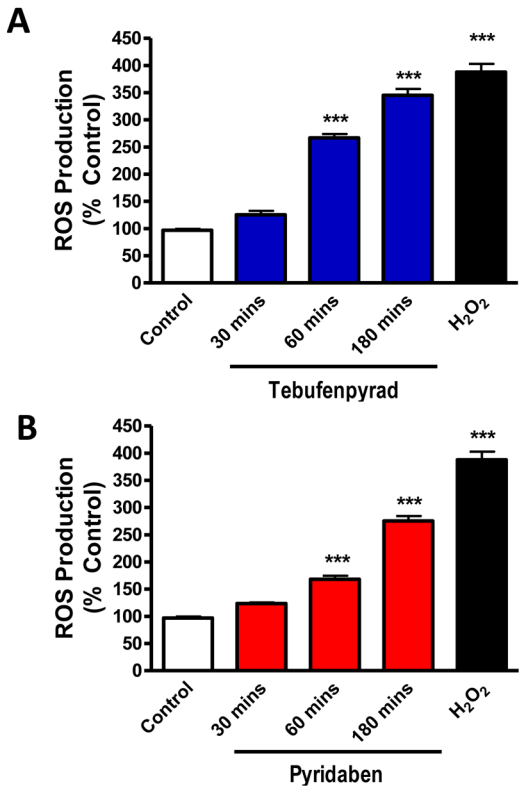

Figure 2. Tebufenpyrad and Pyridaben increased ROS generation in a time-dependent manner

N27 cells were exposed to 3 μM of tebufenpyrad (A) and pyridaben (B) for 30, 60 and 180 min. Cells were then assayed for intracellular ROS production using H_2-DCFDA dye. Hydrogen peroxide (100 μM for 45 min) was used as a positive control. Asterisks ***$p < 0.001$ for control vs treated groups, represented as the mean ± S.E. of three separate experiments performed in hexaplicate.

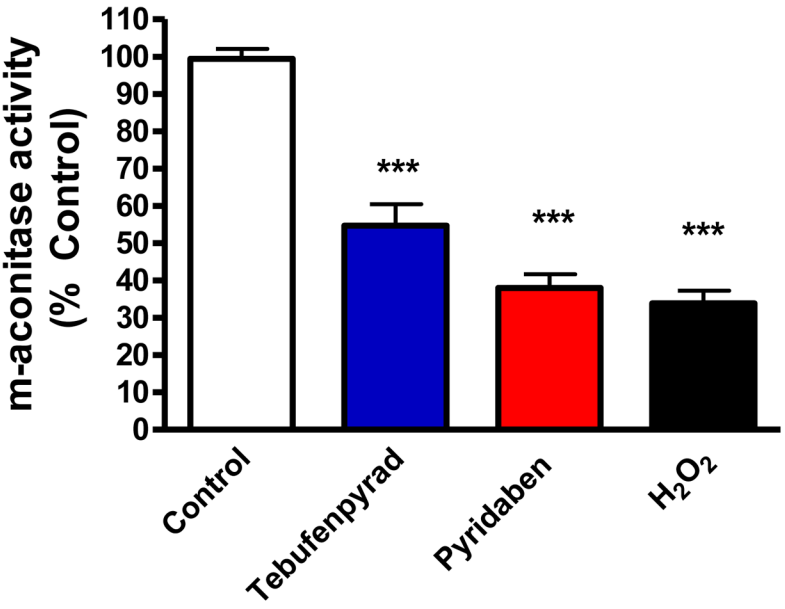

Figure 3. Effect of tebufenpyrad and pyridaben on mitochondrial aconitase enzyme activity in N27 dopaminergic cells

N27 cells were treated with 3 μM of tebufenpyrad and pyridaben for 3 h in serum-free RPMI media. Aconitase activity was measured post-exposure using an aconitase activity kit. Hydrogen peroxide (100 μM) treatment for 45 min was used as a positive control. Aconitase activity is expressed as a percentage of controls. Asterisks ***$p < 0.001$ for control vs treated groups, represented as the mean ± S.E. of three separate experiments performed in hexaplicate.

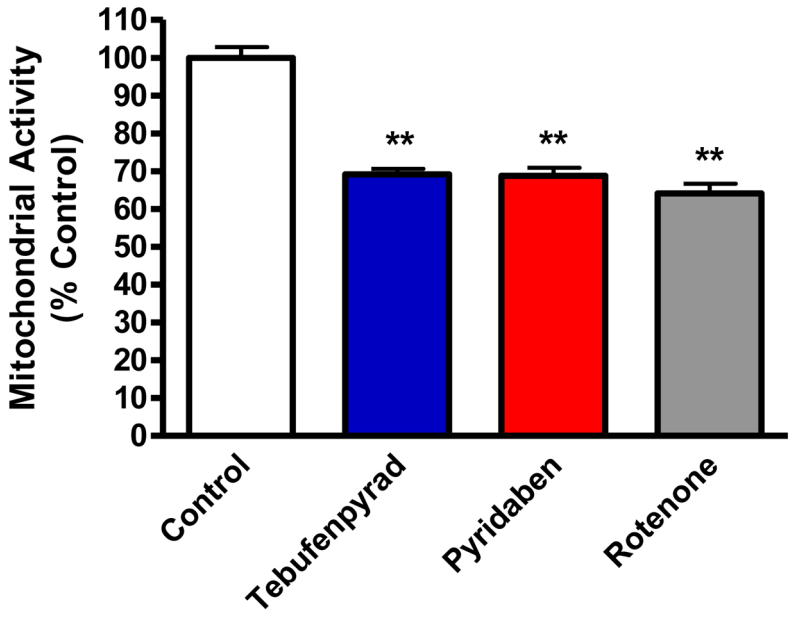

Figure 4. Effect of tebufenpyrad and pyridaben on mitochondrial function in N27 dopaminergic cells

N27 cells were treated with 3 μM of tebufenpyrad and pyridaben for 3 h and assayed for mitochondrial function using the MitoTracker green dye assay. Rotenone (1 μM for 3 h) was used as a positive control. After treatment and incubation with the MitoTracker green dye, readings were taken using a plate reader at an excitation wavelength of 485 nm and an emission wavelength of 520 nm. Values are expressed as relative mitochondrial activity. Asterisks **$p < 0.01$ for control versus treated groups, represented as the mean ± S.E. of three separate experiments performed in hexaplicate.

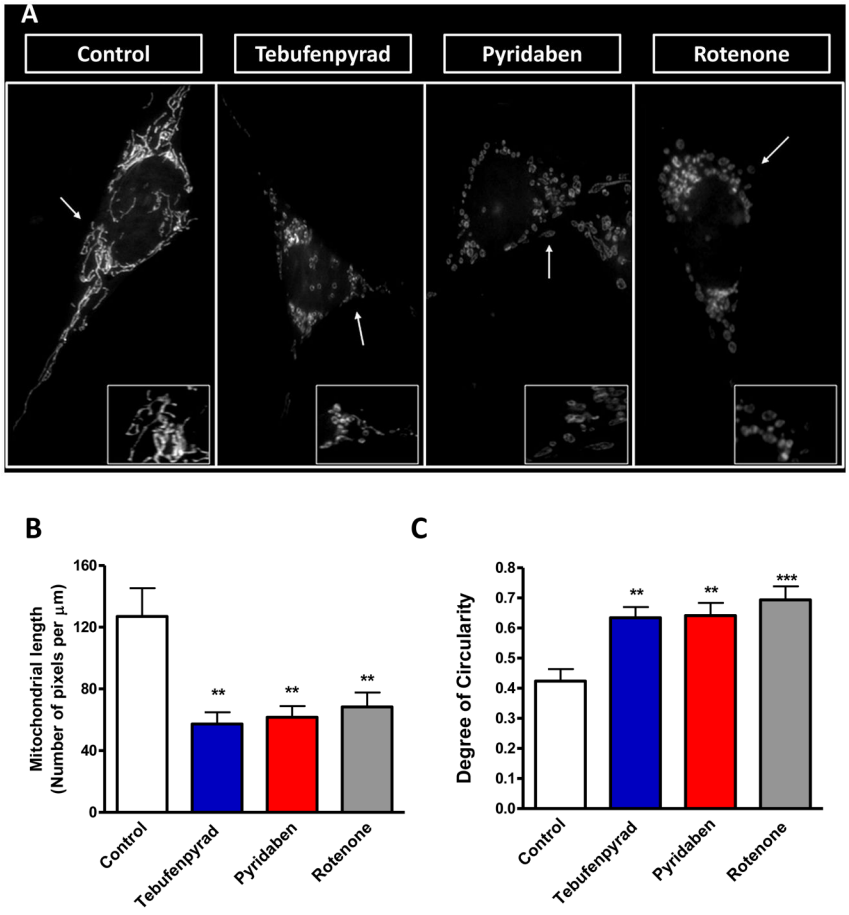

Figure 5. Tebufenpyrad and pyridaben induced significant structural damage to the mitochondria of N27 cells

(A) N27 cells were exposed to 3 μM tebufenpyrad and pyridaben for 3 h. Rotenone (1 μM for 3 h) was used as a positive control. Structural changes to mitochondria were then stained by MitoTracker red dye. Images were obtained using a confocal microscope (60 X magnification). Mitochondrial length (B) and degree of circularity (C) were quantified using ImageJ. Asterisks **$p < 0.01$ and ***$p < 0.001$ for control versus pesticide-treated groups, represented as the mean ± S.E. of two separate experiments performed in hexaplicate.

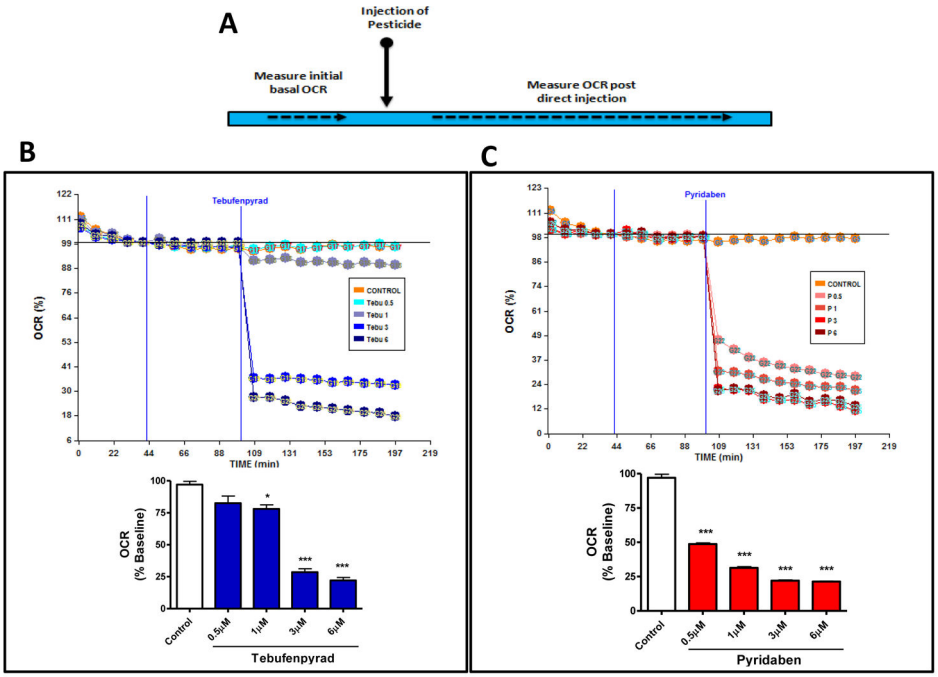

Figure 6. Direct injection of tebufenpyrad and pyridaben to N27 cells leads to plummeting oxygen consumption rates (OCR)

(A) Schematic representation of direct injection method was employed to analyze instantaneous effects on N27 dopaminergic cells after injecting different concentrations of tebufenpyrad and pyridaben. N27 cells grown in a V7-PS culture plate one day prior to the treatment were injected with different concentrations of tebufenpyrad and pyridaben (0.5, 1, 3 and 6 μM) under serum-free conditions. Immediately post-injection, the OCR value was measured using the Seahorse XF96 analyzer. (B and C) Quantification of the output OCR post-injection. Asterisks *$p < 0.05$ and ***$p < 0.001$ for control versus treatment groups, represented as the mean ± S.E. of two separate experiments performed in quadruplicate.

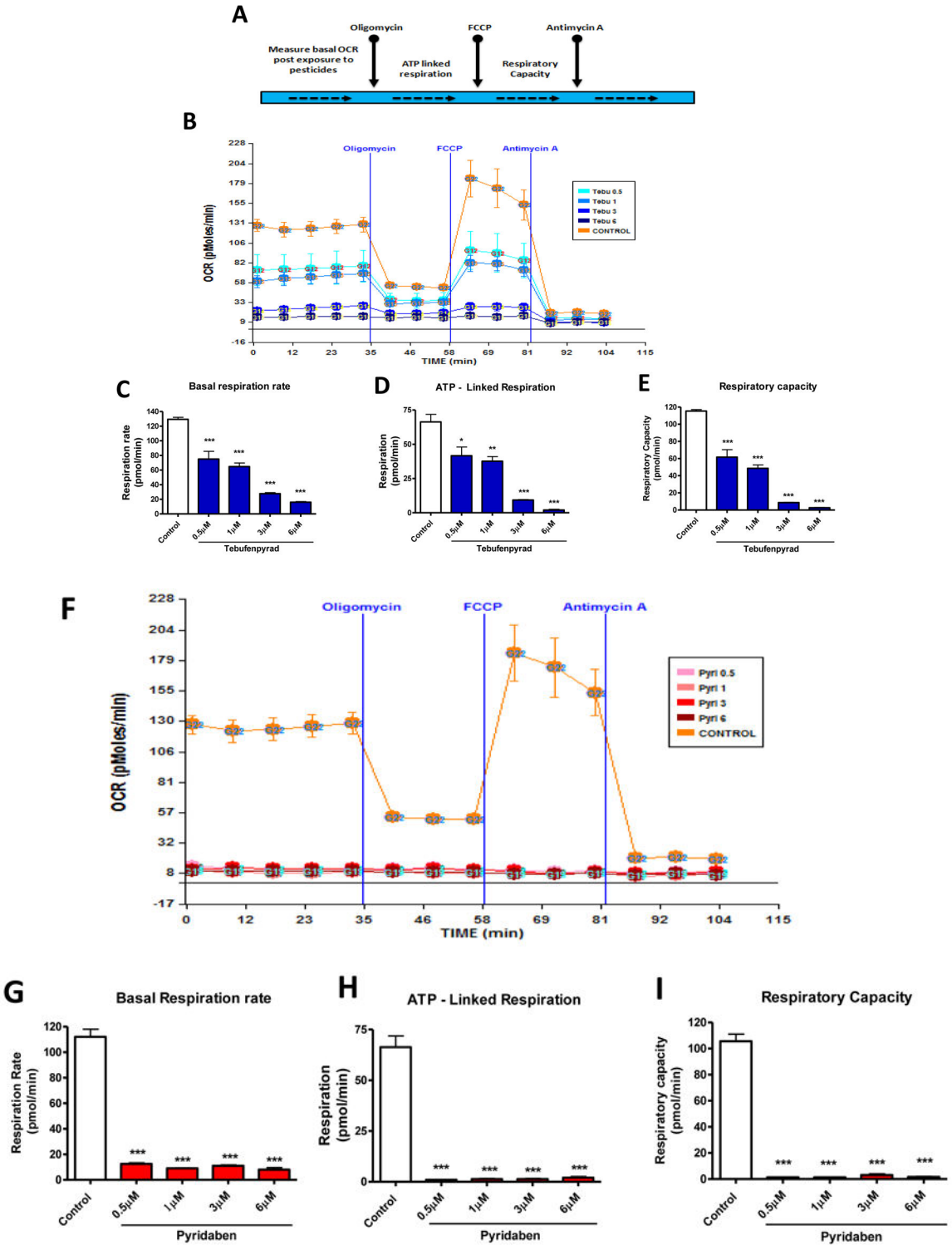

Figure 7. Effect of tebufenpyrad and pyridaben on mitochondrial stress level in N27 dopaminergic cells

(A) Schematic representation of the bioenergetics study to measure and analyze the dose-related effects of tebufenpyrad and pyridaben on mitochondrial dynamics in N27 cells. The

dopaminergic neuronal cells were incubated with different concentrations of tebufenpyrad or pyridaben (0.5, 1, 3 and 6 μM) in serum-free RPMI for 3 h and then the plate was de-gassed and made ready for the OCR measurement using the Seahorse XF96 analyzer. Mitochondrial dynamics were measured using three-stage injection of mito-stressors. Stage 1 injected 1 μg/ml oligomycin, Stage 2 injected 1 μM FCCP and Stage 3 injected 10 μM antimycin A (see Figs. 7B and F). Throughout these stages the analyzer continuously measures OCR. (C–E) Different parameters like basal respiration, ATP-linked respiration and respiratory capacity were estimated from the output OCR values after completion. (G–I) Experiments were repeated under the same conditions with pyridaben. Asterisks ***$p < 0.001$ for control versus treatment groups, represented as the mean ± S.E. of two separate experiments performed in quadruplicate.

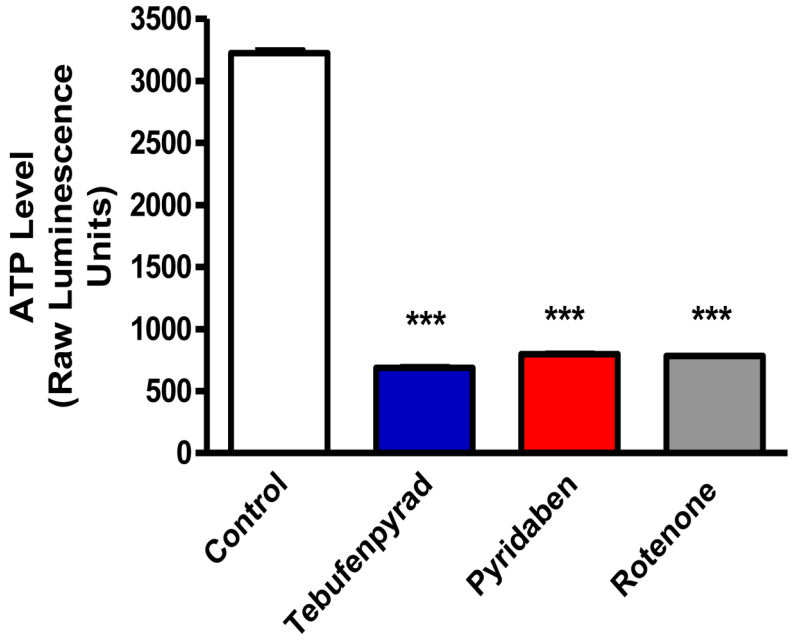

Figure 8. Tebufenpyrad and pyridaben treatment significantly reduced cellular ATP production in N27 dopaminergic cells

N27 cells were exposed to 3 μM of tebufenpyrad or pyridaben for 3 h in serum-free RPMI media. Cell viability was measured with respect to the amount of cellular ATP produced using the Luminescent Cell Viability assay kit and was represented as raw luminescence units (RLU). Rotenone (1 μM for 3 h) was used as a positive control. Asterisks ***$p < 0.001$ for control versus treated groups, represented as the mean ± S.E. of three separate experiments performed in hexaplicate.